NEUROSCIENCE
RESEARCH ARTICLE
K. Y. Lee et al. / Neuroscience 515 (2023) 25–36

Astrocyte-mediated Transduction of Muscle Fiber Contractions Synchronizes Hippocampal Neuronal Network Development

Ki Yun Lee, [a,c] **Justin S. Rhodes** [b,c*] **and M. Taher A. Saif** [a,c,d*]

[a] *Department of Mechanical Science and Engineering, University of Illinois at Urbana-Champaign, Urbana, IL 61801, USA*

[b] *Department of Psychology, University of Illinois at Urbana-Champaign, Urbana, IL 61801, USA*

[c] *Beckman Institute for Advanced Science and Technology, University of Illinois at Urbana-Champaign, Urbana, IL 61801, USA*

[d] *Department of Bioengineering, University of Illinois at Urbana-Champaign, Urbana, IL 61801, USA*

Abstract—Exercise supports brain health in part by enhancing hippocampal function. The leading hypothesis is that muscles release factors when they contract (e.g., lactate, myokines, growth factors) that enter circulation and reach the brain where they enhance plasticity (e.g., increase neurogenesis and synaptogenesis). However, it remains unknown how the muscle signals are transduced by the hippocampal cells to modulate network activity and synaptic development. Thus, we established an *in vitro* model in which the media from contracting primary muscle cells (CM) is applied to developing primary hippocampal cell cultures on a microelectrode array. We found that the hippocampal neuronal network matures more rapidly (as indicated by synapse development and synchronous neuronal activity) when exposed to CM than regular media (RM). This was accompanied by a 4.4- and 1.4-fold increase in the proliferation of astrocytes and neurons, respectively. Further, experiments established that factors released by astrocytes inhibit neuronal hyper-excitability induced by muscle media, and facilitate network development. Results provide new insight into how exercise may support hippocampal function by regulating astrocyte proliferation and subsequent taming of neuronal activity into an integrated network.

Key words: Exercise, muscle, hippocampus, neuronal maturation, neural network, neurogenesis, synaptogenesis, astrogliogenesis, *in vitro* model.

INTRODUCTION

Exercise is a highly effective strategy for maintaining cognitive health throughout life, even when initiated at late stages in life (Churchill et al., 2002; Erickson and Kramer, 2009; Erickson et al., 2011). Many studies have shown robust long-term changes in the hippocampus from increased physical activity, such as increased adult hippocampal neurogenesis, synaptogenesis, and enlarged hippocampal volume which likely support enhanced cognition (van Praag et al., 1999; Redila and Christie, 2006; Clark et al., 2009, 2011; Erickson et al., 2011). However, the mechanisms by which exercise produces such dramatic changes in the hippocampus remain elusive. Uncovering the mechanisms that are responsible for enlarging the hippocampus and enhancing its function could be used to reverse-engineer treatments for cognitive pathologies that result in a diminished size and function of the hippocampus, such as Alzheimer's disease, stress, depression, anxiety, PTSD, Cushing's disease, epilepsy, and normal aging (Dhikav and Anand, 2007).

Cumulative research over the past few decades has suggested that factors released from contracting muscles such as lactate (el Hayek et al., 2019), growth factors (Trejo et al., 2001; Fabel et al., 2003), trophic factors (Church et al., 2016), and myokines (Wrann et al., 2013; Moon et al., 2016) provide crucial signals that support enhanced plasticity (Delezie and Handschin, 2018). However, how muscle factors affect hippocampal cells is still being worked out. Recently, we found that repeated electrical contractions of the hindlimb muscles of anesthetized mice in a pattern that produced endurance adaptations in the muscles (40 reps, twice a week for 8 weeks) caused increased numbers of new astrocytes in the hippocampus and enlarged the volume of the dentate gyrus by approximately 10% (Gardner et al., 2020). This suggests astrocytes are sensitive to muscle factors and proliferate when they detect muscle factors in the blood. Given the role that astrocytes play in forming the blood–

*Corresponding authors.
E-mail addresses: kiyunyl2@illinois.edu (K. Y. Lee), jrhodes@illinois.edu (J. S. Rhodes), saif@illinois.edu (M. Taher A. Saif).

Abbreviations: Ast-CM, Media taken from mixed astrocyte/neuron culture exposed to CM; Ast-RM, Media taken from mixed astrocyte/neuron culture exposed to RM; BTS, N-benzyl-p-toluene sulphonamide; CM, Contracting muscle-conditioned media; MEA, Microelectrode array; RM, Regular media.

https://doi.org/10.1016/j.neuroscience.2023.01.028
0306-4522/

brain barrier, they are well situated to transduce signals from the blood into the brain.

One way to study the interactions between contracting muscle cells and hippocampal cells including neurons and astrocytes is to isolate the cells and perform experiments *in vitro*. For example, previous *in vitro* studies found that muscle-conditioned media attracted neurites of spinal cord motor neurons to form neuro-muscular junctions (McCaig, 1986). Along this line, our lab has been examining cross-talk between muscles and neurons *in vitro.* We recently found that when media from contracting muscle fibers derived from a C2C12 mouse myoblast cell line is applied to neuronal cultures derived from a mouse embryonic stem cell line plated on a micro-electrode array, it enhanced overall neural firing rates of the neurons (Aydin et al., 2020).

To further explore how factors from contracting muscles might influence hippocampal cells, we developed an *in vitro* preparation in which primary mouse skeletal muscle cells are plated on a functionalized substrate. The myoblasts develop bundles of myotubes and begin to contract spontaneously. We then take the media surrounding the contracting muscles (conditioned media, CM) and apply that media to *in vitro* primary hippocampal cell cultures that include neurons and astrocytes. The objectives of this study were to determine whether CM influences the function and maturation of hippocampal neuronal networks, and to investigate the role of astrocytes in the process of transduction of muscle contractions to the activity of hippocampal neuronal networks *in vitro*.

EXPERIMENTAL PROCEDURES

Primary mouse skeletal muscle and hippocampus dissection

Muscle tissues were isolated from the hindlimbs of 4-week-old CD1 mice. We used a total of 6 mice and did not differentiate by sex. The muscle tissue was collected and dissociated using a standard protocol (Wang et al., 2017) with slight modifications. Briefly, the tissues were collected in cold PBS (Corning), minced, and digested for 30 minutes in digestion media consisting of DMEM, 2.5% HEPES, 1% GlutaMAX (all from Gibco), and 1% Penicillin-Streptomycin (Lonza) with the addition of 400 unit/ml collagenase (Worthington) and 2.4 unit/ml dispase (Sigma). The remaining tissues were triturated by pipetting in 0.25% trypsin (Gibco), then filtered by 70 and 40 μm cell strainers. After the dissociation, the pre-plating technique (Rando and Blau, 1994; Qu et al., 1998) was implemented to remove fibroblasts and increase the yield of myoblasts. First, the dissociated cells were plated and incubated in uncoated flasks for three hours. Second, the supernatant with floating cells was collected and transferred into functionalized culture dishes.

For hippocampal dissection, hippocampal tissues were isolated from 2-day-old CD1 mouse pups. We used between 5 and 15 pups for each experiment described below. The hippocampus was dissected and dissociated into single cells following an established protocol (Seibenhener and Wooten, 2012). The dissected hippocampal tissues were collected in cold Hibernate-E (Gibco), minced, then digested twice in 2 mg/ml papain (Sigma) for 30 minutes. The remaining tissues were mechanically dissociated further by pipetting, then filtered by 70 and 40 μm cell strainers.

All procedures were approved by the University of Illinois Institutional Animal Care and Use Committee and adhered to NIH guidelines (protocol number: 21053).

Cell culture

Culture dishes were coated with 0.1 mg/ml Matrigel (Corning). The primary skeletal myoblasts were seeded onto the plates at a density of 0.04 million cells/cm^2. The cells were maintained below 70–80% confluency in muscle growth media consisting of Ham's F-10 Nutrient Mix, 20% fetal bovine serum, 1% GlutaMAX, 1% MEM Non-Essential Amino Acids (all from Gibco), 1% Penicillin-Streptomycin, and 0.5% chick embryo extract (US Biological) with ice-cold 10 ng/ml bFGF, 20 μM forskolin, and 100 μM IBMX (all reagent from Sigma). Once the confluency reached 70–80%, then the culture was maintained in muscle differentiation media consisting of DMEM and Ham's F-12 Nutrient Mix at a volume ratio of 1:1, 10% horse serum, 1% GlutaMAX (all from Gibco), and 1% Penicillin-Streptomycin to initiate myotube formations. Once myotubes were matured and contractions were observed, the media was changed with pre-muscle-conditioned media consisting of Advanced DMEM/F-12, 1% GlutaMAX (all from Gibco), and 1% Penicillin-Streptomycin.

For the hippocampal neuron culture, the preparation of cell culture is the same as muscle culture. Cells were seeded onto the culture plates at a density of 0.04 (for measuring astrocyte numbers) or 0.1 million cells/cm^2 (for measuring numbers of neurons and synapses). This difference was helpful since at the higher seeding density, astrocytes proliferate to the point where they are highly overlapping and difficult to count, whereas neurons are rarer in the cultures. For MEA, we used a higher seeding density of 0.4 million cells/cm^2 which is preferable to obtain a robust neuronal network. For measuring astrocyte numbers in response to the glia inhibitor, we used 0.4 million cells/cm^2 since this was a part of and consistent with MEA studies. Hippocampal neuron cells were cultured using specially formulated media by the lab such as RM, CM, astrocyte media conditioned by RM (Ast-RM), and astrocyte media conditioned by CM (Ast-CM) depending on experiments (see details in Collection of CM, RM, Ast-CM, and Ast-RM).

Muscle anti-actomyosin and glia anti-mitotic treatments

In one experiment below where indicated, the contraction of the muscle cells was inhibited by adding 10 μM *N*-benzyl-*p*-toluene sulphonamide (BTS) (Sigma) prior to collection of CM, that is hereafter referred to as BTS-CM following published methods (Cheung et al., 2002; Pinniger et al., 2005).

In specific experiments below where indicated, the proliferation of glia was inhibited using a standard protocol (Liu et al., 2013). Briefly, the culture was treated with a cocktail consisting of 20 μM 5-fluorodeoxyuridine (MP Biomedicals), 20 μM uridine, and 0.5 μM Arabinofuranosyl Cytidine (all from Sigma) on day 1 and incubated for 72 hours. After 72 hours, 2/3 of the media was replenished with new media without the cocktail. A day after, the whole media was changed without the cocktail.

Collection of CM, RM, Ast-CM, and Ast-RM

Once myotubes were matured and 10–20% of myotubes began to twitch autonomously, approximately 4 days in muscle differentiation media (see above), the media was switched back to pre-muscle-conditioned media. The pre-muscle-conditioned media with the contracting myotubes was collected using 0.22 μm filters every 24 hours for 8 days and stored at −80 °C. For the control, pre-muscle-conditioned media was collected from a culture dish without muscle cells, treated, incubated, and stored the same way as with muscle cells. The final forms of RM and CM consisted of these media combined with Neurobasal medium at a volume ratio of 1:1, 10% KnockOut serum replacement, 1% GlutaMAX (all from Gibco), and 1% Penicillin-Streptomycin with ice-cold 0.1 mM β-mercaptoethanol (Gibco), 10 ng/ml glial-derived neurotrophic factor (Neuromics), and 10 ng/ml ciliary neurotrophic factor (Sigma).

For the collection of Ast-RM and Ast-CM, primary hippocampal neurons and astrocytes were cultured in basal media consisting of Advanced DMEM/F-12 and Neurobasal medium at a volume ratio of 1:1 10% KnockOut serum replacement, 1% GlutaMAX, and 1% Penicillin-Streptomycin. Once the confluency reached 100%, the media was replenished with RM or CM for the collection of Ast-RM or Ast-CM, respectively. The media was collected using 0.22 μm filters every 24 hours and stored at −80 °C.

Immunofluorescence

Immunocytochemistry was performed as follows. Samples were fixed with 4% paraformaldehyde, permeabilized with 0.05% Triton-X for 15 minutes at room temperature, and blocked with a buffer solution consisting of PBS, 5% goat serum (Sigma), and 1% bovine serum albumin (Sigma), and stored overnight at 4 °C. The samples were treated with primary antibodies overnight at 4 °C, secondary antibodies for 2 hours, and DAPI (1:1000; Invitrogen, D1306) for 20 minutes at room temperature.

Primary antibodies were anti-Synaptophysin monoclonal rabbit (1:1000; Abcam, ab32127), anti-PSD95 monoclonal mouse (1:1000; Invitrogen, MA1-046), anti-Bassoon monoclonal mouse (1:1000; Abcam, ab82958), anti-β III Tubulin polyclonal rabbit (1:1000; SYSY, 302 302), anti-NeuN monoclonal mouse (1:1000; Abcam, ab104224), anti-S100β polyclonal chicken (1:1000; SYSY, 287 006), and Alexa Fluor 647-conjugated Phalloidin F-actin (1:500; Invitrogen, A22287). Secondary antibodies were goat anti-chicken IgY Alexa Fluor 488 (ab150173), goat anti-mouse IgY Alexa Fluor 488 (ab150117), goat anti-rabbit IgY Alexa Fluor 568 (ab175696), and goat anti-mouse IgY Alexa Fluor 647 (ab150119) (all 1:500; Abcam).

Immunofluorescent image analysis

All samples were imaged using a Zeiss 710 confocal microscope (Carl Zeiss Microscopy). To detect and measure synapses, synaptic vesicle accumulation, and filamentous actin at presynaptic terminals, the double-fluorescent label method was used following a published protocol with some modifications (Dzyubenko et al., 2016). To count the number of synapses and measure the intensity of synaptic vesicle clustering, we used co-localization of the presynaptic marker, Synaptophysin, and postsynaptic marker, PSD95. Co-labeled puncta that consisted of at least one pixel were counted automatically by removing the background using a fixed threshold. For the intensity of F-actin at the synapse, we used co-localization of F-actin with the Bassoon, presynaptic marker. The total area illuminating double fluorescent markers above a threshold level of intensity was measured in 10 randomly selected regions on the culture plate, each field of view was 0.12 mm^2 (1 pixel = 0.69 μm). The analysis was performed by ImageJ.

A similar analysis was performed to measure the total number of astrocytes and neurons in the culture plates. A comparison of cell numbers between different time points was used to measure astrogliogenesis and neurogenesis in response to the treatments. Note that here we are defining neurogenesis as the appearance of additional neurons in the culture. These additional neurons could be produced from progenitor cells plated when the culture was seeded and subsequently differentiated into neurons or could be from cell division and subsequent differentiation within the culture. To measure number of astrocytes and neurons in the culture dishes, 10 and 20 randomly selected regions, 0.12 (1 pixel = 0.69 μm) and 2.0 mm^2 size (1 pixel = 2.77 μm), were analyzed, respectively. A cell was automatically counted as an astrocyte if it displayed at least 30 pixels of co-labeling between DAPI and S100β relative to a fixed threshold level of intensity for each marker. A cell was counted as a neuron if it displayed at least 8 pixels co-labeling between DAPI and NeuN. For the analysis of number of astrocytes in response to the glia inhibitor, 9 randomly selected regions, 0.5 mm^2 size (1 pixel = 1.38 μm) each, were analyzed, and an astrocyte was counted if at least 7.5 pixels of co-labeling occurred between DAPI and S100β. These different sampling and co-labeling methods for the different analyses were used because the seeding densities were different, and because of the different density of the cell types in the culture dishes. In all cases, the automatic detection methods were validated by observing the particles that were counted in images.

Calcium Imaging

Calcium imaging was performed using Cal-590-AM (AAT Bioquest, 20510) by the manufacturer's protocols. Briefly,

samples were incubated with DMEM, 0.04% Pluronic F-127 (Sigma), and 5 μM Cal-590-AM for an hour at 37 °C. After washout, samples were supplemented with DMEM with no phenol red to reduce background noise. The dye-loaded cells were excited at 574 nm and imaging was performed at the frame rate of 12 fps. For quantitative analysis, the average fluorescence intensity of selected regions of interest was calculated. Then the trace of fluorescent dynamics was calculated as $\Delta F/F_0 = (F_n - F_0)/F_0$, where F_n and F_0 are the average intensity at n^{th} frame and at the resting state, respectively.

MEA preparation

MEA measurements were performed using an MEA 2,100-Lite Amplifier (Multi Channel Systems MCS GmbH). The 6-well MEA device was fabricated by a manufacturer (Multi Channel Systems MCS GmbH), and it contained 9 embedded 30 μm diameter TiN electrodes per well with 200 μm spacing between electrodes and six reference electrodes. The MEA device was coated with 0.1 mg/ml Poly-D-Lysine (Sigma) and Matrigel for cell culture preparation. Measurements were performed at a sampling rate of 10 kHz for 5 min at 37 °C with a sealed cover to keep CO_2 concentration stable. Media was replenished every other day.

MEA recording, and spike/burst detection

Neuronal activity was analyzed by Multi-Channel Analyzer software (Multi Channel Systems MCS GmbH), Python (3.9.7), and MATLAB. Raw data were filtered using a 2nd order Butterworth high pass filter with 200 Hz cutoff frequency. Action potentials were detected as spikes by a threshold of 4 × standard deviations for both rising and falling edge from the noise magnitude distribution. Spikes were only detected by active electrodes which were defined by electrodes containing at least 5 spikes/min. The following criteria were used to define bursts. A burst must consist of at least 4 spikes, last at least 50 ms long, and must be separated from another burst by at least 100 ms. To start and end a burst, the interval between the first two and the last two spikes should be less than 50 ms, respectively.

Synchrony index

The synchrony of spike trains between electrodes was assessed through cross-correlation for discrete functions. There are total of nine electrodes and spike train data for each electrode was cross-correlated with every other electrode. The synchrony index was achieved by averaging 36 possible combinations. The cross-correlation was proceeded with zero lag. The synchrony index, $\bar{\chi}$, of nine electrodes is described as.

$$\bar{\chi} = \frac{1}{36}\sum_{p=1}^{9}\sum_{q=p+1}^{9}\frac{\sum(x_i^p \cdot y_i^q)}{\sqrt{\sum(x_i^p)^2 \cdot \sum(y_i^q)^2}}$$

where x and y are spike trains consisting of 0 (no spike) and 1 (spike), p and q are the p^{th} and q^{th} electrode, and i is the i^{th} discrete time. $\bar{\chi} = 0$ and $\bar{\chi} = 1$ represent completely asynchronous and synchronous, respectively.

Statistical analysis

SAS (9.4) and R (4.0.3) were used for statistical analysis. The number of culture dishes (n) was chosen based on a statistical power analysis to detect an effect size of 10% with an 80% probability. $p < 0.05$ was considered statistically significant. F statistic is provided as $F_{n,\ m}$ where F is a ratio of between-group variance to within-group variance. n and m represent degrees of freedom between- and within-group, respectively. Data were considered normally distributed when the absolute value of the skewness and kurtosis was less than 1 and 2, respectively. In the case of non-normal distribution, a power transform was used to transform data to meet the normality conditions. Muscle contraction amplitude, calcium signal, actin intensity, and astrocyte number in response to the glia inhibitor were evaluated by a two-sample t-test (control vs BTS 10 μM, RM vs CM, and control vs glia inhibitor). Synapse number, vesicle accumulation, astrocyte number, and neuron number were evaluated by two-way ANOVA with day (day 2 or 3 vs day 9) and treatment (RM vs CM) as factors. The MEA outcomes of the BTS study were analyzed using repeated measures three-way ANOVA with the cohort as a blocking variable, day (day 2–9) entered as a within-subjects, muscle treatment (2 levels: RM vs CM) as a between-subjects factor, and drug (2 levels: control vs BTS) entered as a between-subjects factor. Similarly, the MEA outcomes of the glia-reduced study were analyzed using repeated measures three-way ANOVA with the cohort as a blocking variable, day (day 2-9), muscle treatment (2 levels: RM vs CM), and astrocyte composition (3 levels: presence vs absence vs absence with astrocyte releasate). For the burst rate (BTS and glia-reduced study) and synchrony index (glia-reduced study), aligned rank transform was used for the non-parametric test since data were considered non-normally distributed. Post-hoc pairwise differences between means were performed using Fisher's least significant difference test.

RESULTS

Contracting muscle-conditioned media enhances neuronal activity measured by microelectrode arrays

Consistent with our previous MEA study with C2C12 mouse myoblast cell line and mouse embryonic stem cell-derived neuronal culture (Aydin et al., 2020), CM from primary skeletal muscle cells increased spike and burst rates of primary hippocampal neurons across days (Fig. 1A and 1B). The general pattern of development of spike trains over time in RM was consistent with other studies using primary hippocampal cells and primary sensory neurons at a similar cell seeding density (Biffi et al., 2013; Black et al., 2018). Significant differences in spike rates were observed between days ($F_{7,\ 80} = 19.4$, $p < 0.001$) and between RM versus CM treatments ($F_{1,\ 80} = 202.2$, $p < 0.001$). The interaction between day

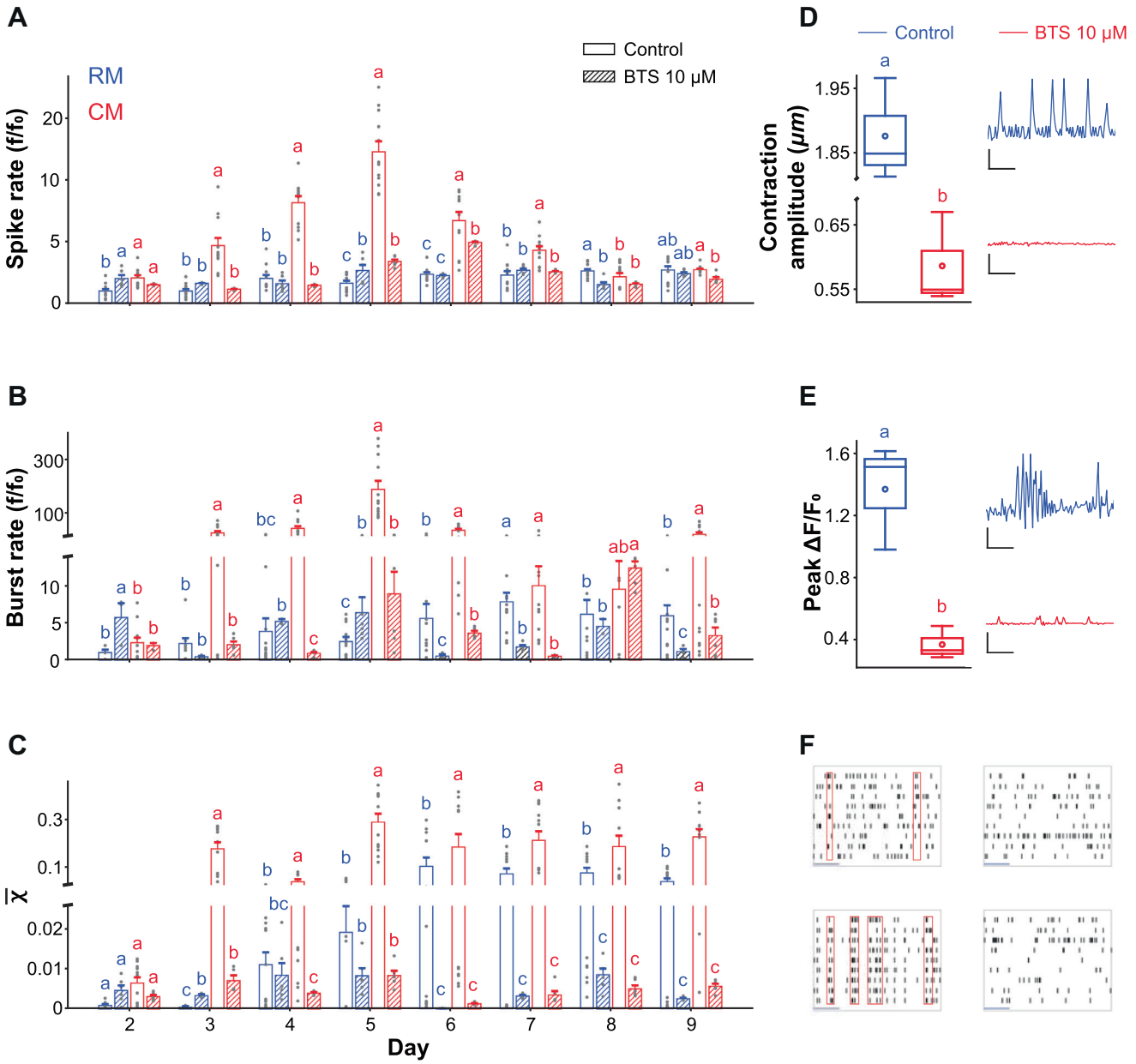

Fig. 1. Muscle contraction-conditioned media increases hippocampal neuronal activity. (A) Primary mouse hippocampal cells were cultured on a multi-electrode array (MEA) for 9 days with the following treatments: regular media (RM), muscle contraction-conditioned media (CM), RM with N-benzyl-p-toluene sulphonamide (BTS-RM), CM with BTS (BTS-CM). Average number of spikes per second (±SEM) across all electrodes normalized to the average value for RM on day 2 are shown. **(B)** Average number of bursts per minute normalized to the average value for RM on day 2. **(C)** Average synchrony index (n = 12 for control and 6 for BTS cultures). Different lowercase letters above bar plots indicate significant differences among treatments within each day ($p < 0.05$). **(D)** Average muscle contraction amplitudes between control and 10 μM BTS (left). Skeletal muscle contraction patterns in the presence of 0 (top right) and 10 μM BTS (bottom right). Scale bar in x, y = 1 s, 1 μm. **(E)** Peak fluorescent changes between control and 10 μM BTS (n = 3). Traces of calcium dynamics in the presence of 0 (top right) and 10 μM BTS (bottom right). Scale bar in x, y = 2 s, 1 $\Delta F/F_0$. Different lowercase letters above box plots indicate significant differences between treatments ($p < 0.05$). **(F)** Raster plots representing spike trains from nine electrodes from RM (top left), RM with BTS (top right), CM (bottom left), and CM with BTS (bottom right) on day 9. Each line and the red box represent a single firing, and synchronous burst, respectively. Scale bar = 2 s.

and treatment was also significant ($F_{7,\ 80}$ = 23.7, $p < 0.001$). Similar to spike rate, burst rate also showed significant effects of day ($F_{7,\ 72}$ = 10.5, $p < 0.001$), treatment ($F_{1,\ 72}$ = 38.3, $p < 0.001$), and interaction between the two ($F_{7,\ 72}$ = 21.1, $p < 0.001$). The interactions were caused by a different pattern of results for earlier time points (days 2–7), as compared to later time points (days 8 and 9). At the early time points, CM had a higher spike and burst rates, but at later time points the difference in them between RM and CM was reduced, absent, or reversed.

Similar to spike rate and burst rate, CM also caused neurons to fire more synchronously as compared to RM (Fig. 1C). A two-way ANOVA showed a significant effect of day ($F_{7,\ 75}$ = 175.7, $p < 0.001$), treatment ($F_{1,\ 75}$ = 4083.4, $p < 0.001$) and the interaction between

the two ($F_{7, 75}$ = 231.1, p < 0.001). However, unlike spike rate and burst rate which showed greater differences between CM and RM at initial time points than later time points, the synchrony index showed the reverse pattern, with greater differences at the later time points and no difference at the early time points when little synchronous firing occurred.

Having shown that CM increases spike rate, burst rate and synchronous firing of primary hippocampal neurons in culture, we next wanted to evaluate whether contraction of the muscles was necessary for the MEA effects. The alternative is that muscle cells release neuro-active factors regardless of whether they are contracting. Hence, we repeated the experiment except we treated the muscle cells with a contraction inhibitor before collecting the media. We used a known skeletal muscle myosin II inhibitor, N-benzyl-p-toluene sulphonamide (BTS). BTS weakens myosin's interaction with F-actin and *ex vivo* studies found 10 μM of BTS suppresses force production by 60% (Cheung et al., 2002; Pinniger et al., 2005). Consistent with these results, the amplitudes of muscle contraction were reduced by 69% with BTS *in vitro* (t_4 = 20.7, p < 0.001; Fig. 1D). Moreover, we performed calcium imaging of the skeletal muscles *in vitro* (see details in Experimental procedures). Calcium dynamics in muscle cultures show a 73% reduction between control and 10 μM of BTS (t_4 = 4.9, p = 0.0083; Fig. 1E). Widefield (Videos S1 and S2) and calcium imaging (Videos S3 and S4) of skeletal muscles are available as supplementary materials.

BTS prevented CM from increasing spike and burst rate, but had no effect on baseline spike and burst rate in RM. This suggests muscle cell contractions are required for CM to increase spike and burst rate. For spike and burst rate, all factors in the repeated measures ANOVA were significant including day ($F_{7, 212}$ = 50.2, p < 0.001; $F_{7, 187}$ = 24.3, p < 0.001), muscle treatment (RM vs CM) ($F_{1, 31}$ = 194.0, p < 0.001; $F_{1, 21}$ = 48.8, p < 0.001), BTS treatment ($F_{1, 31}$ = 101.2, p < 0.001; $F_{1, 21}$ = 52.8, p < 0.001) and all interactions (all p < 0.001). Post-hoc comparisons showed no difference between RM and BTS-RM (p = 0.4516; p = 0.1607), whereas CM produced greater spike and burst rates as compared to BTS-CM (p < 0.001, p < 0.001). Finally, BTS-CM was not different from RM (p = 0.1272, p = 0.9548) or BTS-RM (p = 0.4553; p = 0.1643).

While BTS specifically reduced spike and burst rate in CM with no effect on RM, we observed a different result for the synchrony index. BTS completely obliterated the synchrony index when added to either RM or CM treatments. This was supported by a significant effect of day, muscle treatment, BTS treatment and all interactions in the overall repeated measures ANOVA. Post-hoc tests showed that BTS-RM and BTS-CM displayed near zero synchrony across the entire period. The synchrony indices in BTS-RM and BTS-CM groups were significantly lower than in RM (p < 0.001, p < 0.001) and in CM without BTS (p < 0.001, p < 0.001) collapsed across days. Taken together, this suggests BTS has a direct effect on the cell culture preventing synchrony and hence we cannot draw strong conclusions about whether contraction of muscles is required for increasing the synchrony index without further experimentation.

Contracting muscle-conditioned media promotes synaptogenesis

Primary hippocampal cells plated in culture form synapses over a period of days. An increased number or strength of synapses could explain the increased synchrony index in CM compared to RM. To quantify synaptic development in response to CM versus RM, we performed immunocytochemistry to count the number of synapses using co-localization of pre- and post-synaptic markers (see details in Experimental procedures) on days 2 and 9 for CM and RM (Dzyubenko et al., 2016).

The results showed that CM expedites synaptic development compared to RM. This was supported by a significant effect of day ($F_{1, 20}$ = 19.6, p < 0.001), no main effect of treatment (RM vs CM) ($F_{1, 20}$ = 0.77, p = 0.3896), but a significant interaction between day and treatment ($F_{1, 20}$ = 8.5, p = 0.0087; Fig. 2A). Post-hoc tests indicated a significant increase in the synapse number from day 2 to 9 in RM (p < 0.001), but not in CM (p = 0.2953). On day 2, the synapse number in CM was significantly higher by 44% compared to that in RM (p = 0.0145), but on day 9, no differences between CM and RM were detected (p = 0.1669). The confocal images of post-synapses, synaptic vesicles, and colocalization are shown in supplementary materials (Fig. S1).

Contracting muscle-conditioned media accrues filamentous actin at presynaptic terminals but does not significantly affect vesicle clustering

Functional synapses display an accumulation of vesicles and filamentous actin at the terminals (Fletcher et al., 1991). F-actin plays a critical role in clustering and transporting vesicles within the synapse (Pieribone et al., 1995; Kim and Lisman, 1999; Pechstein and Shupliakov, 2010; Peng et al., 2012). Hence, we wanted to determine whether CM affected vesicle accumulation and filamentous actin concentration at the synapse as a potential mechanism for the increased neuronal activity and synchrony observed in CM (Fig. 1A–C).

Following established methods (Dzyubenko et al., 2016) to quantify neurotransmitter vesicle clustering at the synapse, we measured the average intensity of Synaptophysin, a transmembrane protein for vesicles, co-localized with PSD95, postsynaptic nerve terminal marker. Also, we measured the average intensity of F-actin, co-localized with Bassoon, presynaptic nerve terminal marker. Results indicated vesicle clustering occurred at a similar rate in CM and RM. The ANOVA indicated a significant effect of day ($F_{1, 20}$ = 7.6, p = 0.0121), but no main effect of treatment ($F_{1, 20}$ = 1.1, p = 0.2990) or interaction ($F_{1, 20}$ = 0.79, p = 0.3844; Fig. 2B). On day 2, F-actin was not detected in either CM or RM, so results are not shown. However, filamentous actin was

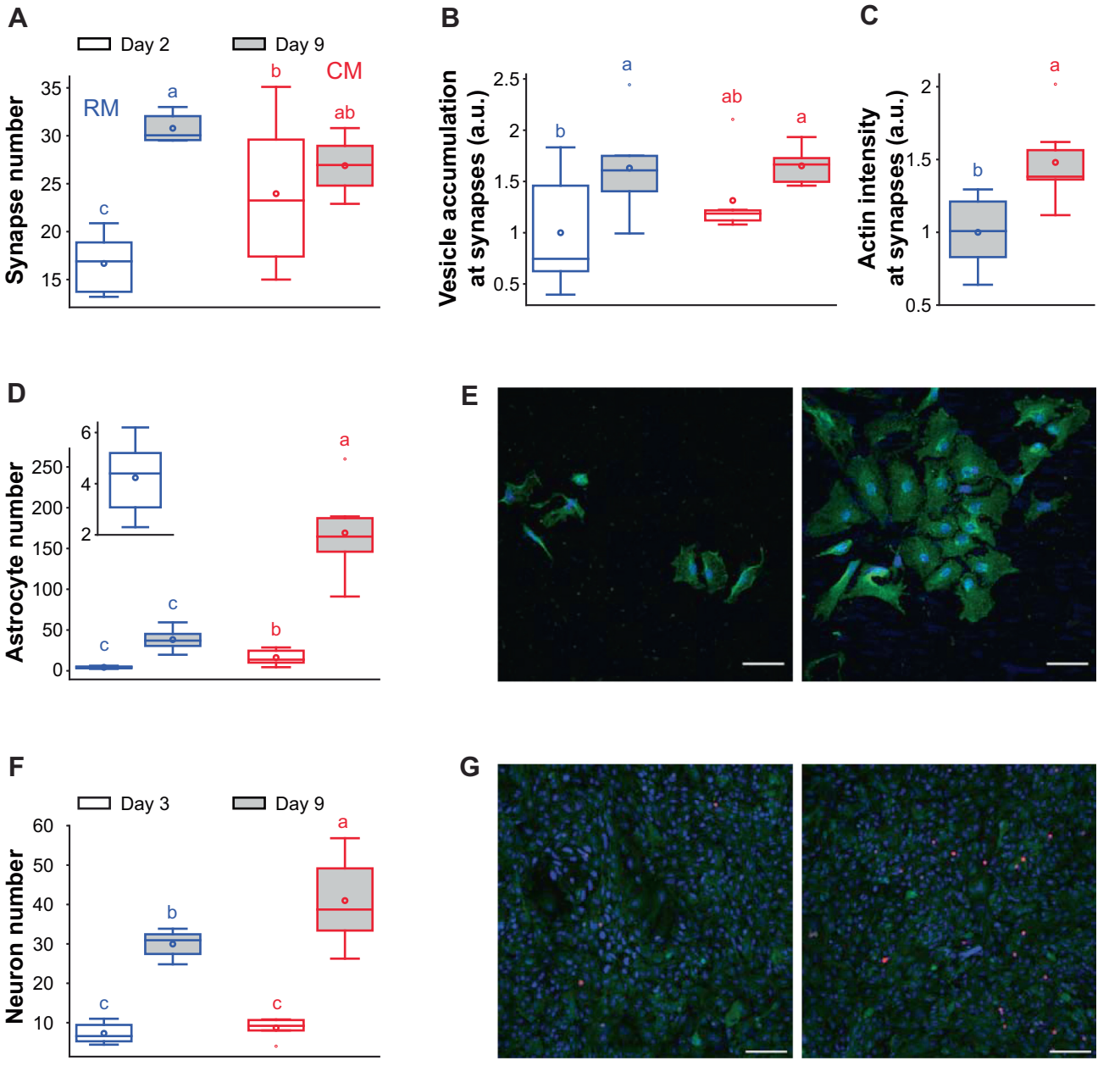

Fig. 2. Muscle contraction-conditioned media accelerates hippocampal neuron synapse development (A) Primary mouse hippocampal cells were cultured for 9 days with regular media (RM) or muscle contraction-conditioned media (CM). Average number of synapses (±SEM), as measured by immunohistochemical detection of pre and postsynaptic markers, are shown for RM and CM on days 2 and 9. **(B)** Average vesicle accumulation per synapse on days 2 and 9. Data are shown normalized to the average value for RM on day 2. **(C)** Average F-actin intensity on day 9 (F-actin levels were below the limit of detection on day 2). Data are shown normalized to the average value for RM. **(D)** Average number of astrocytes on days 2 and 9. The inset shows RM on day 2 on a smaller scale ($n = 6$ per group). **(E)** Images of astrocytes in the cultures on day 2 in RM (left) and CM (right) (S100β, green; DAPI, blue). Scale bar = 50 μm. **(F)** Average number of neurons on day 3 and 9 ($n = 6$ for day 3 and $n = 8$ for day 9). **(G)** Images of neurons and astrocytes in the cultures on day 9 in RM (left) and CM (right) (NeuN, red; S100β, green; DAPI, blue). Scale bar = 100 μm. Different lowercase letters above box plots indicate significant differences between treatments and days ($p < 0.05$).

detected on day 9 in both groups, and the average F-actin intensity in CM was higher by 48% ($t_{10} = 2.9$, $p = 0.0152$; Fig. 2C). Example confocal images of F-actin along with Synaptophysin and Bassoon for synapse identification and DAPI for reference are shown in supplementary materials (Fig. S2).

Muscle-conditioned media from contracting muscles induces astrocyte proliferation

To quantify astrogliogenesis, cells expressing S100β were counted. The number of astrocytes increased by 9.0-fold in RM and 10.4-fold in CM from day 2 to 9 indicating significant astrogliogenesis in culture over

days (Fig. 2D). CM displayed 3.8- and 4.4-fold greater numbers of astrocytes than RM on day 2 and 9, respectively. This was reflected by a significant effect of day ($F_{1, 20} = 145.0$, $p < 0.001$) and treatment ($F_{1, 20} = 49.1$, $p < 0.001$) but no interaction ($F_{1, 20} = 0.93$, $p = 0.3466$). This suggests CM massively increases the proliferation of hippocampal astrocytes similar to the effect observed *in vivo* (Gardner et al., 2020).

Muscle-conditioned media from contracting muscles induces neurogenesis

Here we define neurogenesis as the addition of new mature neurons in the culture dish. Neurogenesis was measured by counting NeuN-positive cells in cultures from day 3 to 9. Note, as mentioned above, increased neurons on day 9 as compared to day 3 could be caused by neural progenitor cells that were seeded in the culture and subsequently differentiated into neurons or from proliferating neural progenitor or stem cells. The number of neurons increased by 4.1-fold in RM and 4.7-fold in CM from day 3 to day 9, indicating neurogenesis occurred in the culture dishes. Post-hoc tests indicated no significant difference in the number of neurons between RM and CM on day 3 ($p = 0.63$), but CM displayed approximately 40% more neurons than RM on day 9 ($p = 0.0014$) (Fig. 2F). This was reflected by a significant effect of day ($F_{1, 19} = 180.5$, $p < 0.001$), treatment ($F_{1, 19} = 8.6$, $p = 0.0086$), and interaction ($F_{1, 19} = 5.5$, $p = 0.0295$). Confocal images showing NeuN, with β Tubulin as an alternate marker of neurons, along with S100β (astrocyte marker) and DAPI for reference are shown in supplementary materials (Fig. S3).

Astrocytes regulate neuronal activity *in vitro*

To determine how increased astrocytes (Fig. 2D) may have contributed to the increased spike rate observed in response to CM versus RM, we repeated the MEA experiment in cultures with reduced astrocyte populations. To remove astrocytes from the primary hippocampal cell culture, we applied a glia inhibitor following established protocols (Liu et al., 2013) (see details in Experimental procedures). Consistent with previous accounts, this resulted in an 81% reduction in the number of astrocytes in the culture ($t_{14} = 5.70$, $p < 0.001$) (Fig. 3A). Confocal images of astrocyte populations in control and astrocyte-reduced cultures are shown in Fig. 3B.

MEA data were collected from normal hippocampal cultures in RM and CM as reference controls, as well as from cultures with reduced astrocytes in RM, CM, Ast-RM, and Ast-CM (see details in Experimental procedures). In the repeated measures analysis of mean spike rate, all main effects of muscle-conditioned media (RM vs CM) ($F_{1, 53} = 254.8$, $p < 0.001$), presence or absence of astrocytes ($F_{2, 53} = 170.6$, $p < 0.001$), and day ($F_{7, 364} = 131.7$, $p < 0.001$) were significant, and all possible interactions between these factors were also significant ($p < 0.001$). The presence or absence of astrocyte factors includes 3 levels, presence, absence, and absence but with the releasate from astrocytes added back in (Ast-RM and Ast-CM groups; see Statistical analysis). Post-hoc tests indicated that CM increased spike rate relative to RM in normal hippocampal cultures consistent with the previous result ($p < 0.001$), but also in cultures with reduced astrocytes ($p < 0.001$). To our surprise, we found that a reduction of astrocytes increased the spike rate in both RM and CM ($p < 0.001$), and the increase in CM with reduced astrocytes was an order of magnitude higher compared to the unaltered culture in CM (Fig. 3C). Moreover, the increase in spike rate in CM relative to RM was greater for cultures with reduced astrocytes as compared to unaltered cultures as reflected by the significant interaction between muscle media and presence/absence of astrocytes ($F_{2, 53} = 49.8$, $p < 0.001$). Taken together, these results suggest astrocytes inhibit neuronal activity and CM increases their inhibitory function to counteract the excitatory effect of CM on neuronal activity.

The spike rates in the Ast-groups were similar to when the astrocytes were physically present in intact primary hippocampal cultures. This is supported by a non-significant post-hoc test between groups where astrocytes were physically present versus absent but releasate added back in ($p = 0.0537$). Further, comparisons between normal cultures exposed to CM and astrocyte-deprived cultures exposed to Ast-CM showed no significant difference ($p = 0.96$). Likewise, normal cultures exposed to RM showed no difference from astrocyte-deprived cultures with Ast-RM ($p = 0.68$). These results suggest that astrocytes mediate their inhibitory effect by releasing factors into the media and do not need to be physically present in the culture to exert their influence.

DISCUSSION

Here we establish for the first time an *in vitro* platform to explore interactions between contracting primary muscle cells and primary hippocampal cells. One of the leading hypothesized mechanisms for pro-cognitive effects of exercise is that muscle contractions release factors that cross into the brain where they directly influence hippocampal cells involved in cognition (van Praag et al., 1999; Trejo et al., 2001; Wrann et al., 2013). This hypothesis is supported by our recent discovery that muscle contractions alone, through electrical stimulation of the sciatic nerve in anesthetized mice, are capable of increasing the generation of new astrocytes in the hippocampus and increasing the volume of the dentate gyrus (Gardner et al., 2020). The *in vitro* model developed herein adds to this literature by identifying a novel mechanism by which muscle cells may communicate with hippocampal cells. Muscle cells release factors that cause hippocampal neurons to become excited and to form functional synapses. The factors also cause neurogenesis, and astrogliogenesis. Furthermore, the expanded astrocytes appear to play a critical role in regulating neuronal excitability. Together this leads to a network that develops earlier and has overall greater excitability than in absence of the muscle sig-

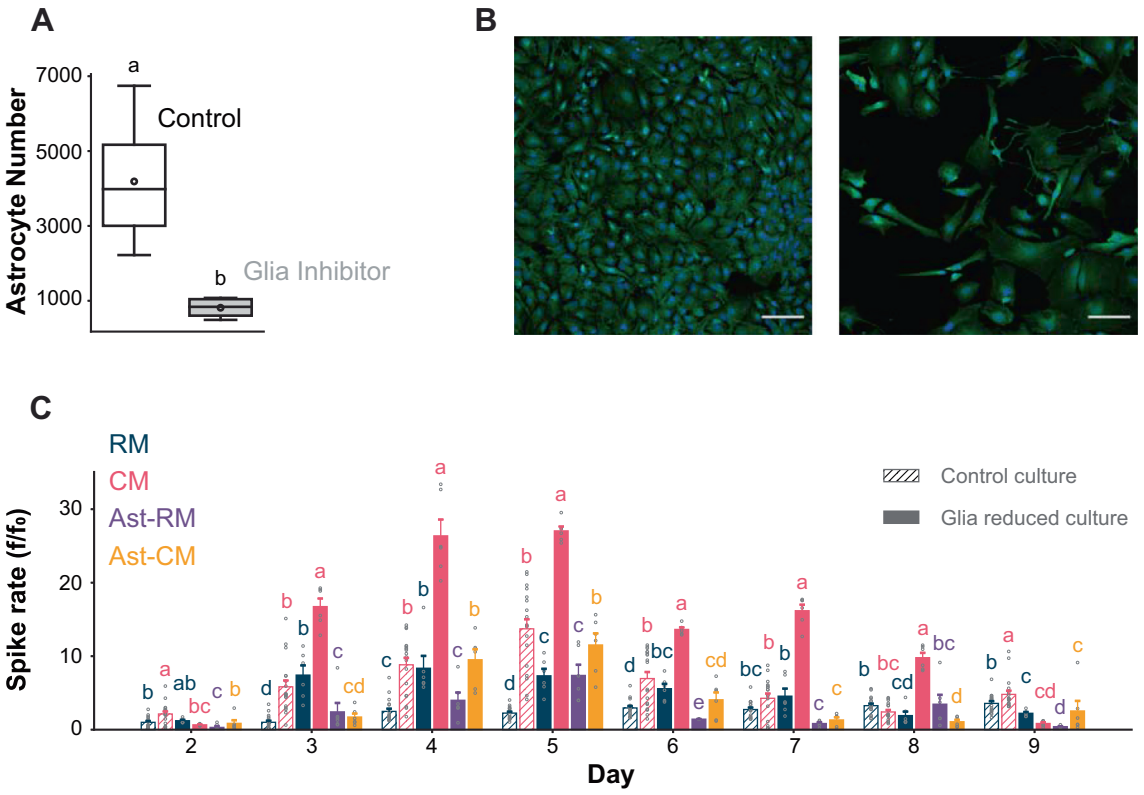

Fig. 3. Astrocytes release factors that tame muscle-media-induced neuronal activity (A) Average number of astrocytes in control and glia-reduced group on day 4 ($n = 8$). **(B)** Images of the control and glia-reduced cultures on day 4 (S100β, green; DAPI, blue). Scale bar = 100 μm. **(C)** Average number of spikes per second (±SEM) normalized to RM on day 2 in the presence and absence of astrocytes ($n = 18$ for control and 6 for glia-reduced cultures). Different lowercase letters above bar plots indicate significant differences among treatments and cultures within each day ($p < 0.05$). Results for burst rate and synchrony index are shown in supplementary materials (Fig. S4 and Appendix S1).

nals, but also greater inhibition from astrocytes. The astrocytes thus tame the increased electrical activation of the circuit from the muscle factors in a way that leads to a selective strengthening of coordinated activation patterns between neurons.

Astrocytes are well-known homeostatic regulators of neuronal activity. They directly modulate the ratio of excitatory and inhibitory synapses and neurotransmitter concentrations such as GABA and glutamate based on environmental needs (Li et al., 1999). When astrocyte-conditioned media was supplemented in astrocyte-deprived situations, increases in GABAergic synapses, axon length (Hughes et al., 2010), and receptors (Diniz et al., 2014) were detected. In the context of whole organismal exercise, muscles communicate with the hippocampus while hippocampal cells are involved in the sensorimotor processing involved in physical activity (Saraulli et al., 2017; Delezie and Handschin, 2018). Indeed, acute activation of the hippocampus is strongly correlated with running speed and repeated exercise training which results in adult hippocampal neurogenesis and astrogliogenesis (van Praag et al., 1999; Redila and Christie, 2006; Clark et al., 2009; Erickson et al., 2011). Together with the *in vitro* data collected herein, the results suggest that muscle contractions contribute to the plasticity in the hippocampus by responding with signals that increase the number of new astrocytes to counterbalance the excitation that is likely intrinsic to the hippocampus involved in the sensorimotor response to physical activity.

In addition to taming the excitation of hippocampal neurons, the increased number of astrocytes may have contributed to the increased maturation of the hippocampal network by strengthening specific synapses and weakening others by pruning and inhibition. Mature synapses appeared earlier and were pruned earlier in cultures with more astrocytes as a consequence of exposure to CM. Whereas synapses continued to increase from day 2 to day 9 in RM, in CM they reached their peak around day 2 and were already in decline by day 9 (Fig. 2A). Moreover, F-actin was more concentrated at presynaptic terminals in CM than in RM on day 9 (Fig. 2C). F-actin is known to be concentrated at presynaptic terminals to support the vesicles (Pieribone et al., 1995; Pechstein and Shupliakov, 2010; Peng et al., 2012) and to mediate their transportation (Kim and Lisman, 1999). Together, this could explain why neuronal cultures plated on MEA exposed to CM displayed greater levels of synchronized firings of action potentials than RM because there were more mature functional synapses. Astrocyte-secreted proteins such as thrombospondins (Christopherson et al., 2005), hevin, and SPARC (Kucukdereli et al., 2011) may have promoted synaptogenesis. Astrocytes can also directly eliminate synapses through MEGF10

and MERTK pathways which are two phagocytic receptors detecting signals from silent synapses (Chung et al., 2013, 2015).

A key finding was that muscle contractions are necessary for CM to influence spike rate and burst rate in the hippocampal cultures. When muscles were prevented from contracting by administering BTS, CM no longer produced the increased effects on spike and burst rate (Fig. 1A and 1B). This adds important validity to the model since exercise involves mechanical forces and the hypothesis is that muscle contractions release factors that they otherwise would not release to communicate their status of engaging in physical activity to the hippocampus. We were able to make this conclusion because the effect of BTS on spike and burst rate was specific to CM, it had no impact when administered in RM, (i.e., BTS-RM spike and burst rate was similar to RM, but BTS-CM showed reduced spike and burst rate relative to CM). However, this was not true for the synchrony index where BTS appeared to directly eliminate synchronous firing of neurons whether in RM or CM (Fig. 1C). Thus, we cannot be certain that the muscle contractions are necessary for the effect of CM on enhancing synchronous firing of action potentials. A method is needed that can prevent the muscle cells from contracting that does not directly interfere with any of the MEA outcomes.

One of the big differences between the *in vitro* model and the whole organism is that in the whole organism, the blood–brain barrier (BBB) controls which factors in the blood reach the brain, whereas in the *in vitro* model the muscle factors are released directly onto the brain cells. Our understanding of how the BBB filters myokines and other molecules is incomplete. We know astrocytic processes form the BBB, and hence astrocytes would be the first cells in the brain to receive signals from the blood. Hence, the large response we observed for astrocytes is perhaps consistent with this role. In any event, the *in vitro* model is only useful insofar is it recapitulates key features of the whole organismal phenomenon. In our case, the exposure of the hippocampal cells to the muscle media reproduces the whole organismal phenomenon of exercise-induced neuronal activity, synaptogenesis, astrogliogenesis, and neurogenesis. This means there are likely similar mechanisms at play in both systems.

While we established CM increases neurogenesis, as defined by the appearance of additional mature neurons in the culture from day 3 to day 9 in CM than RM, we noted that this result could have been caused by progenitor cells originally seeded and subsequently surviving and differentiating into neurons after day 3, rather than from increased proliferation of progenitor cells. Exercise increases neurogenesis *in vivo* mainly by increasing the survival and differentiation of proliferating cells rather than by increasing proliferation (Clark et al., 2010). Thus, the difference between control and treatment groups (RM vs CM) is not expected to occur from proliferation but rather a difference in survival and differentiation of cells that have already proliferated. On the other hand, the large increase in number of neurons from day 3 to day 9 is likely not only attributed to differentiation of originally plated progenitor cells but cell division and proliferation of progenitor cells in culture. Future studies are needed to determine the cause of the increased mature neurons in CM than RM whether by increased proliferation and/or survival and differentiation as occurs during normal exercise in rodents.

Future studies will build on the *in vitro* platform to explore potential reciprocal communication between muscle cells and hippocampal cells through a co-culture with shared media exchange. We are also interested in using the platform to explore the potential mechanism by which CM causes astrocytes to proliferate and hippocampal networks to mature faster. In addition, we are interested in tracking other cell types such as microglia that may play a role in the network maturation, in particular synaptic pruning (Paolicelli et al., 2011). Finally, we are interested in identifying the bio-active factors released from the contracting muscles that influence the hippocampal cultures. In the future, such information could be used to reverse engineer treatments to recapitulate pro-cognitive effects of exercise in the absence of physical activity.

ACKNOWLEDGEMENTS

We are grateful to Dr. Gelson Pagan-Diaz of the University of Texas for discussions of MEA, Jennie Gardner for husbandry of animal subjects and mouse muscle dissections at the early stage of the study, Md Saddam Hossain Joy for discussions of the double-fluorescent label method, Carlos Renteria for discussions of calcium imaging and MATLAB code, Meghan Connolly for discussions of neurogenesis, and Dr. Onur Aydin of the University of Illinois for ideations and overall insightful discussions of the study. Personally, I (KYL) appreciate my mother, Young Me Heo for moral support through weekly phone calls.

DECLARATION OF INTEREST

All authors declare no conflicts of interest in this work.

FUNDING

This work was supported by the National Institutes of Health (R21 NS109894), and National Science Foundation (CMMI 1935181).

REFERENCES

Aydin O, Passaro AP, Elhebeary M, Pagan-Diaz GJ, Fan A, Nuethong S, Bashir R, Stice SL, Saif MTA (2020) Development of 3D neuromuscular bioactuators. APL Bioeng 4.

Biffi E, Regalia G, Menegon A, Ferrigno G, Pedrocchi A (2013) The influence of neuronal density and maturation on network activity of hippocampal cell cultures: A methodological study. PLoS One 8.

Black BJ, Atmaramani R, Kumaraju R, Plagens S, Romero-Ortega M, Dussor G, Price TJ, Campbell ZT, Pancrazio JJ (2018) Adult mouse sensory neurons on microelectrode arrays exhibit increased spontaneous and stimulus-evoked activity in the presence of interleukin-6. J Neurophysiol 120.

Cheung A, Dantzig JA, Hollingworth S, Baylor SM, Goldman YE, Mitchinson TJ, Straight AF (2002) A small-molecule inhibitor of skeletal muscle myosin II. Nat Cell Biol 4.
Christopherson KS, Ullian EM, Stokes CCA, Mullowney CE, Hell JW, Agah A, Lawler J, Mosher DF, Bornstein P, Barres BA (2005) Thrombospondins are astrocyte-secreted proteins that promote CNS synaptogenesis. Cell 120.
Chung WS, Clarke LE, Wang GX, Stafford BK, Sher A, Chakraborty C, Joung J, Foo LC, Thompson A, Chen C, Smith SJ, Barres BA (2013) Astrocytes mediate synapse elimination through MEGF10 and MERTK pathways. Nature 504.
Chung WS, Allen NJ, Eroglu C (2015) Astrocytes control synapse formation, function, and elimination. Cold Spring Harb Perspect Biol 7.
Church DD, Hoffman JR, Mangine GT, Jajtner AR, Townsend JR, Beyer KS, Wang R, la Monica MB, Fukuda DH, Stout JR (2016) Comparison of high-intensity vs. high-volume resistance training on the BDNF response to exercise. J Appl Physiol 121.
Churchill JD, Galvez R, Colcombe S, Swain RA, Kramer AF, Greenough WT (2002) Exercise, experience and the aging brain. Neurobiol Aging 23.
Clark PJ, Brzezinska WJ, Puchalski EK, Krone DA, Rhodes JS (2009) Functional analysis of neurovascular adaptations to exercise in the dentate gyrus of young adult mice associated with cognitive gain. Hippocampus 19.
Clark PJ, Kohman RA, Miller DS, Bhattacharya TK, Haferkamp EH, Rhodes JS (2010) Adult hippocampal neurogenesis and c-Fos induction during escalation of voluntary wheel running in C57BL/6J mice. Behav Brain Res 213.
Clark PJ, Kohman RA, Miller DS, Bhattacharya TK, Brzezinska WJ, Rhodes JS (2011) Genetic influences on exercise-induced adult hippocampal neurogenesis across 12 divergent mouse strains. Genes Brain Behav 10.
Delezie J, Handschin C (2018) Endocrine crosstalk between Skeletal muscle and the brain. Front Neurol 9.
Dhikav V, Anand KS (2007) Is hippocampal atrophy a future drug target? Med Hypotheses 68.
Diniz LP, Tortelli V, Garcia MN, Araújo APB, Melo HM, Seixas da Silva GS, de Felice FG, Alves-Leon SV, de Souza JM, Romão LF, Castro NG, Gomes FCA (2014) Astrocyte transforming growth factor beta 1 promotes inhibitory synapse formation via CaM kinase II signaling. Glia 62.
Dzyubenko E, Rozenberg A, Hermann DM, Faissner A (2016) Colocalization of synapse marker proteins evaluated by STED-microscopy reveals patterns of neuronal synapse distribution in vitro. J Neurosci Methods 273.
el Hayek L, Khalifeh M, Zibara V, Abi Assaad R, Emmanuel N, Karnib N, El-Ghandour R, Nasrallah P, Bilen M, Ibrahim P, Younes J, Abou Haidar E, Barmo N, Jabre V, Stephan JS, Sleiman SF (2019) Lactate mediates the effects of exercise on learning and memory through sirt1-dependent activation of hippocampal brain-derived neurotrophic factor (BDNF). J Neurosci 39.
Erickson KI, Kramer AF (2009) Aerobic exercise effects on cognitive and neural plasticity in older adults. Br J Sports Med 43.
Erickson KI, Voss MW, Prakash RS, Basak C, Szabo A, Chaddock L, Kim JS, Heo S, Alves H, White SM, Wojcicki TR, Mailey E, Vieira VJ, Martin SA, Pence BD, Woods JA, McAuley E, Kramer AF (2011) Exercise training increases size of hippocampus and improves memory. Proc Natl Acad Sci U S A 108.
Fabel K, Fabel K, Tam B, Kaufer D, Baiker A, Simmons N, Kuo CJ, Palmer TD (2003) VEGF is necessary for exercise-induced adult hippocampal neurogenesis. Eur J Neurosci 18.
Fletcher TL, Cameron P, de Camilli P, Banker G (1991) The distribution of synapsin I and synaptophysin in hippocampal neurons developing in culture. J Neurosci 11.
Gardner JC, Dvoretskiy SV, Yang Y, Venkataraman S, Lange DA, Li S, Boppart AL, Kim N, Rendeiro C, Boppart MD, Rhodes JS (2020) Electrically stimulated hind limb muscle contractions increase adult hippocampal astrogliogenesis but not neurogenesis or behavioral performance in male C57BL/6J mice. Sci Rep 10.
Hughes EG, Elmariah SB, Balice-Gordon RJ (2010) Astrocyte secreted proteins selectively increase hippocampal GABAergic axon length, branching, and synaptogenesis. Mol Cell Neurosci 43.
Kim CH, Lisman JE (1999) A role of actin filament in synaptic transmission and long-term potentiation. J Neurosci 19.
Kucukdereli H, Allen NJ, Lee AT, Feng A, Ozlu MI, Conatser LM, Chakraborty C, Workman G, Weaver M, Sage EH, Barres BA, Eroglu C (2011) Control of excitatory CNS synaptogenesis by astrocyte-secreted proteins hevin and SPARC. Proc Natl Acad Sci U S A 108.
Li YX, Schaffner AE, Barker JL (1999) Astrocytes regulate the developmental appearance of GABAergic and glutamatergic postsynaptic currents in cultured embryonic rat spinal neurons. Eur J Neurosci 11.
Liu R, Lin G, Xu H (2013) An Efficient Method for Dorsal Root Ganglia Neurons Purification with a One-Time Anti-Mitotic Reagent Treatment. PLoS One 8.
McCaig CD (1986) Myoblasts and myoblast-conditioned medium attract the earliest spinal neurites from frog embryos. J Physiol 375.
Moon HY, Becke A, Berron D, Becker B, Sah N, Benoni G, Janke E, Lubejko ST, Greig NH, Mattison JA, Duzel E, van Praag H (2016) Running-Induced Systemic Cathepsin B Secretion Is Associated with Memory Function. Cell Metab 24.
Paolicelli RC, Bolasco G, Pagani F, Maggi L, Scianni M, Panzanelli P, Giustetto M, Ferreira TA, Guiducci E, Dumas L, Ragozzino D, Gross CT (2011) Synaptic pruning by microglia is necessary for normal brain development. Science 1979:333.
Pechstein A, Shupliakov O (2010) Taking a back seat: Synaptic vesicle clustering in presynaptic terminals. Front Synaptic Neurosci.
Peng A, Rotman Z, Deng PY, Klyachko VA (2012) Differential Motion Dynamics of Synaptic Vesicles Undergoing Spontaneous and Activity-Evoked Endocytosis. Neuron 73.
Pieribone VA, Shupliakov O, Brodin L, Hilfiker-Rothenfluh S, Czernik AJ, Greengard P (1995) Distinct pools of synaptic vesicles in neurotransmitter release. Nature 375.
Pinniger GJ, Bruton JD, Westerblad H, Ranatunga KW (2005) Effects of a myosin-II inhibitor (N-benzyl-p-toluene sulphonamide, BTS) on contractile characteristics of intact fast-twitch mammalian muscle fibres. J Muscle Res Cell Motil 26.
Qu Z, Balkir L, van Deutekom JCT, Robbins PD, Pruchnic R, Huard J (1998) Development of approaches to improve cell survival in myoblast transfer therapy. J Cell Biol 142.
Rando TA, Blau HM (1994) Primary mouse myoblast purification, characterization, and transplantation for cell-mediated gene therapy. J Cell Biol 125.
Redila VA, Christie BR (2006) Exercise-induced changes in dendritic structure and complexity in the adult hippocampal dentate gyrus. Neuroscience 137.
Saraulli D, Costanzi M, Mastrorilli V, Farioli-Vecchioli S (2017) The Long Run: Neuroprotective Effects of Physical Exercise on Adult Neurogenesis from Youth to Old Age. Curr Neuropharmacol 15.

Seibenhener ML, Wooten MW (2012) Isolation and culture of hippocampal neurons from prenatal mice. J Vis Exp.
Trejo JL, Carro E, Torres-Alemán I (2001) Circulating insulin-like growth factor I mediates exercise-induced increases in the number of new neurons in the adult hippocampus. J Neurosci 21.
van Praag H, Kempermann G, Gage FH (1999) Running increases cell proliferation and neurogenesis in the adult mouse dentate gyrus. Nat Neurosci 2.
Wang C, Yue F, Kuang S (2017) Muscle Histology Characterization Using H&E Staining and Muscle Fiber Type Classification Using Immunofluorescence Staining. Bio Protoc 7.
Wrann CD, White JP, Salogiannnis J, Laznik-Bogoslavski D, Wu J, Ma D, Lin JD, Greenberg ME, Spiegelman BM (2013) Exercise induces hippocampal BDNF through a PGC-1α/FNDC5 pathway. Cell Metab 18.

APPENDIX A. SUPPLEMENTARY MATERIAL

Supplementary material to this article can be found online at https://doi.org/10.1016/j.neuroscience.2023.01.028.

(Received 8 October 2022, Accepted 24 January 2023)
(Available online xxxx)